Quantum State Interferography

Surya Narayan Sahoo,[1] Sanchari Chakraborti[1] Arun K. Pati,[2] and Urbasi Sinha[1,*]

[1]*Light and Matter Physics, Raman Research Institute, Bengaluru 560080, India*
[2]*Quantum Information and Computation Group, Harish-Chandra Research Institute,*
HBNI, Allahabad 211019, India

Quantum state tomography (QST) has been the traditional method for characterization of an unknown state. Recently, many direct measurement methods have been implemented to reconstruct the state in a resource efficient way. In this Letter, we present an interferometric method, in which any qubit state, whether mixed or pure, can be inferred from the visibility, phase shift, and average intensity of an interference pattern using a single-shot measurement—hence, we call it quantum state interferography. This provides us with a "black box" approach to quantum state estimation, wherein, between the incidence of the photon and extraction of state information, we are not changing any conditions within the setup, thus giving us a true single shot estimation of the quantum state. In contrast, standard QST requires at least two measurements for pure state qubit and at least three measurements for mixed state qubit reconstruction. We then go on to show that QSI is more resource efficient than QST for quantification of entanglement in pure bipartite qubits. We experimentally implement our method with high fidelity using the polarization degree of freedom of light. An extension of the scheme to pure states involving $d-1$ interferograms for d-dimensional systems is also presented. Thus, the scaling gain is even more dramatic in the qudit scenario for our method, where, in contrast, standard QST, without any assumptions, scales roughly as d^2.

Introduction.—The inherent probabilistic features of quantum measurement play a central role in quantum mechanics. The probability distribution of outcomes of any measurement on a quantum system can be predicted if its quantum state is known. However, an unknown quantum state of a single particle cannot be directly determined in any experiment [1]. Nevertheless, if we have an ensemble of identically prepared particles, we can reconstruct the quantum state by measuring the expectation values of different observables.

One of the widely used methods for state reconstruction is the quantum state tomography (QST) technique [2,3], which often requires additional postprocessing to ensure the physicality of the reconstructed density matrix [4,5]. For a d-dimensional system, typically one requires $d^2 - 1$ measurements to reconstruct an arbitrary state. For a pure qudit state, measurement of $5d - 7$ observables suffices to give us a unique state [6,7]. Over the last decade, several schemes towards improving the scaling of QST with the dimension of the Hilbert space have been suggested [8–10] and recently the focus has been towards single-shot state estimation, i.e., obtaining the state in a single setup without any required change in the experimental settings [11–14].

In this Letter, we present a novel method for reconstructing (pure or mixed) quantum state of a qubit along with its experimental implementation, and also extend the scheme to infer the state of d-dimensional qudits requiring only $d-1$ measurements, which serves as a promising and less cumbersome alternative to QST. We emphasize that in our proposed scheme, the number of measurements scales linearly with the dimensionality of the system whereas, in general, the required number of measurements for QST scales quadratically with respect to the system size. Thus, for higher-dimensional systems, our method is more economical compared to QST. Our method can also be used for quantification and reconstruction of bipartite pure entangled states in an efficient manner.

Earlier, other alternatives to standard QST using projective measurements have been explored, in which the strength of interaction may be strong as in Ref. [15] or weak as in Refs. [16–18]. Since weak measurements [19,20] can give us complex weak values of observables, they have paved the way for direct measurement of quantum state [21–27]. Our work in this Letter focuses on the use of interferometric methods as opposed to direct measurement techniques to obtain the quantum state.

Recently, it has been shown by us [28] and others [29] that complex weak values can be obtained without performing weak measurement, which can lead to efficient direct measurement of quantum states [30]. Knowing the weak value of a Hermitian operator can give us the expectation value of a related non-Hermitian operator [31]. Expectation value of non-Hermitian column operators have been used for direct measurement of the state [32].

In this Letter, we show that interferometric methods can be used to infer the quantum state of an ensemble of

identically prepared qubits by a single-shot measurement [33]. We name our method quantum state interferography (QSI). QSI focuses on minimizing the number of data acquisitions as all parameters describing the state are obtained at once by postprocessing the interference pattern. This differs from direct state measurement which focuses on minimizing postprocessing at the cost of changing the experimental setup. QSI has enormous practical benefits vis-a-vis quantum state estimation that can be useful in various applications like quantum information processing protocols [34,35]. We experimentally implement it in polarization degree of freedom of light, which yields a single-shot method for characterization of the polarization state of light.

Next, we discuss the theory for how a two-path interferometer can be used to reconstruct not only pure states but also mixed states. We then experimentally demonstrate the method using 632.8 nm helium-neon laser light in a displaced Sagnac interferometer [36]. Then, we extend the protocol to qudits and show the advantage of using QSI over QST for pure states.

Quantum state interferography for qubits.—The general density matrix for a qubit can be written using the coordinates $\theta \in [0, \pi]$ and $\phi \in (-\pi, \pi]$, which describe the direction of the vector in the Bloch sphere representation, and $\mu \in [0, 1]$, which is related to the purity of the state and the length of the vector.

$$\rho = \begin{pmatrix} \cos^2\left(\frac{\theta}{2}\right) & \frac{1}{2}\mu e^{-i\phi}\sin(\theta) \\ \frac{1}{2}\mu e^{i\phi}\sin(\theta) & \sin^2\left(\frac{\theta}{2}\right) \end{pmatrix}. \qquad (1)$$

The expectation value of spin-ladder operators $\sigma_\pm = \frac{1}{2}(\sigma_x \pm i\sigma_y)$ is given as

$$\langle\sigma_\pm\rangle = \text{Tr}(\rho\sigma_\pm) = \frac{1}{2}\exp(\pm i\phi)\mu\sin(\theta). \qquad (2)$$

The argument of the complex expectation value $\langle\sigma_\pm\rangle$ directly gives us the azimuthal coordinate, i.e., $\phi = \pm\arg(\langle\sigma_\pm\rangle)$. For a pure state, $\mu = 1$ and hence, the θ can be obtained as $\sin^{-1}(2|\langle\sigma_\pm\rangle|)$. However, the solution to θ is not unique in $[0, \pi]$ and $\pi - \theta$ is a solution as well. Thus, to uniquely determine θ, we need to measure the expectation value of another column operator, which in this case is the projector $\Pi_0 = |0\rangle\langle0|$, with $\langle\Pi_0\rangle = \cos^2(\theta/2)$. Once $\langle\Pi_0\rangle$ is known, θ is uniquely determined in $[0, \pi]$. Now, μ can be determined as $\mu = [2|\langle\sigma_\pm\rangle|/\sin(\theta)]$.

Next, we show that all three quantities θ, ϕ, and μ specifying the polarization state of light can be determined from a single interference pattern obtained in the Mach-Zehnder interferometer (MZI) as shown in Fig. 1. The operator $A = \sigma_-$ is polar decomposed into the $R = \Pi_0$ and $U = \sigma_x$. The optical components corresponding to R and U are placed in each arm of the MZI.
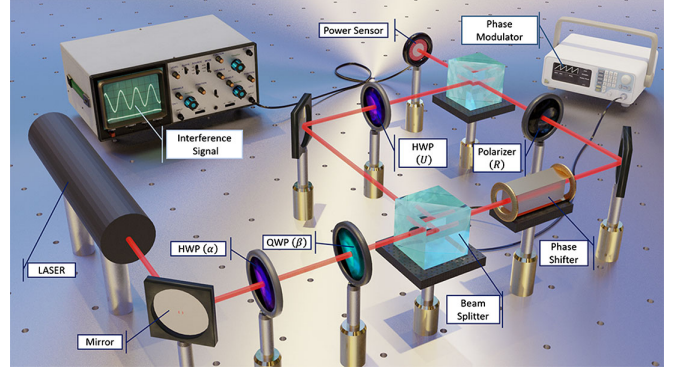

FIG. 1. The polarization state is prepared by using half-wave plate (HWP) and quarter-wave plate (QWP), which can be at arbitrary orientations. The MZI is formed by the two beam splitters (BS). On one arm we place a HWP oriented at $\pi/4$ to realize the σ_x operator. On the other arm, we use a polarizer with transmission axis oriented along the horizontal, or alternatively, the transmitting port of the polarizing beam splitter (PBS) to effectively realize the operator Π_0. The phase shifter introduces a relative phase φ between the two arms and we measure the intensity at the photodetector as a function of φ. Experimentally, the phase shifter can be avoided by making the interferometer noncollinear (See Fig. 2 and Ref. [28]) to obtain the interferogram in a single shot.

We will discuss the scheme by taking an example of a MZI. However, it can be realized with any two-path interferometer including a double-slit interferometer that can be factory designed and can serve as a robust miniature device for state estimation. If a pure state $|\psi\rangle$ is incident
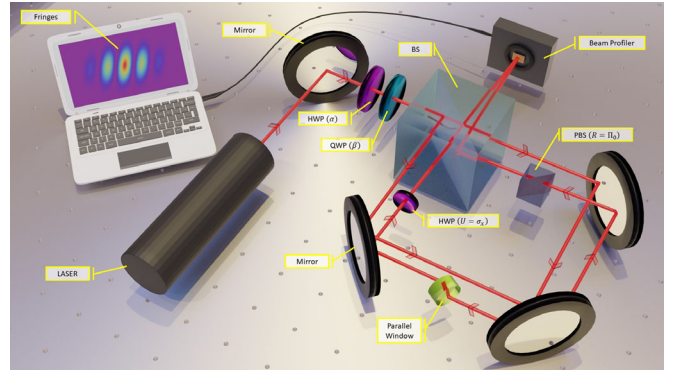

FIG. 2. Noncollinear displaced Sagnac interferometer for polarization state interferography: We use the Sagnac interferometer in noncollinear configuration [28], i.e., we tilt the beam splitter (Thorlabs BS013) to obtain double-slit-like interference pattern. We use the displaced Sagnac configuration [36] instead of the common-path configuration in order to place the polarizing beam splitter (PBS, Thorlabs PBS122) in one arm (as $R = \Pi_0$ operation) and the HWP (Thorlabs WPH05M-633) in the other arm as the $U = \sigma_x$ operation. The glass plate, (parallel window WG40530-B) placed in one of the paths is tilted to achieve the displacement of that beam to ensure maximum overlap of the two noncollinear beams at the beam profiler.

onto the first beam splitter (BS) of a MZI, the intensity at the photodetector [28] is given by

$$I(\varphi) = \frac{1}{4}[1 + \langle \Pi_0 \rangle + 2|\langle \sigma_- \rangle| \cos(\arg(\langle \sigma_- \rangle) + \varphi)]. \quad (3)$$

By knowing $I(\varphi)$, which can be experimentally obtained from a single interference pattern, we can determine $\langle \Pi_0 \rangle$ and $\langle \sigma_- \rangle$.

If the incident state is a mixed state given by ρ, we obtain the intensity at the detector [37] as follows:

$$I(\varphi) = \frac{1}{8}[3 + \cos(\theta) + 2\,\mu\sin(\theta)\cos(\varphi - \phi)]. \quad (4)$$

The phase shift of the interference pattern is obtained at the value of φ that maximizes $I(\varphi)$. Since $0 \le \theta \le \pi \Rightarrow \sin(\theta) > 0$, the phase shift is obtained as $\Phi = \phi$.

The phase averaged intensity and the visibility are given by

$$\bar{I} = \frac{1}{8}[3 + \cos(\theta)], \qquad V = \frac{2\,\mu\sin(\theta)}{3 + \cos(\theta)}, \quad (5)$$

where $\theta \in [0, \pi]$ can be uniquely determined from $\bar{I}$, which is experimentally always normalized with the incident intensity. Once θ is known, μ can be obtained from visibility and ρ can be reconstructed.

Interestingly, QSI can also be used to quantify entanglement of pure bipartite states. If a bipartite state is pure, then entanglement can be quantified by the entanglement entropy—the von Neumman entropy of the reduced density matrix, i.e., $E = -\text{Tr}[\rho_A \log(\rho_A)]$, where $\rho_A = \text{Tr}_B(\rho_{AB})$ and $\rho_{AB} = |\Psi\rangle_{AB}\langle\Psi|_{AB}$ [39–41]. Since, with a single experimental setup the reduced density matrix ρ_A, which in general is a mixed state, can be determined using QSI, it can be used to quantify entanglement of pure states of bipartite qubits. The state $|\Psi\rangle_{AB}$ can be completely

reconstructed with one additional interferogram as we have shown in the Supplemental Material [37].

Experiment.—To reconstruct the state of various input polarizations we need to measure the phase shift of the interference pattern. If one uses a MZI, it needs to be phase stabilized against vibrations that change the path difference. Thus, to avoid this, we prefer interferometers that are not prone to vibrations such as the Sagnac interferometer [37].

The input state is prepared by placing a HWP (Thorlabs WPH05M-633) at an angle α followed by a QWP (Thorlabs WPQ05M-633) at an angle β in the path of a vertically polarized beam from a helium neon laser (632.8 nm) before it enters the interferometer. For a fixed angle α of the HWP, we rotate the QWP and obtain 5 images for a given β. For each image, we take 100 horizontal slices about the vertical centroid and fit each slice with the model that is a Gaussian weighted cosine function:

$$B_f + A_f e^{-c_f(x_f - m_f)^2}[1 + v_f \cos(k_f x_f + \phi_f)]. \quad (6)$$

Here, B_f is the background noise and A_f is the amplitude of the Gaussian envelope centered at m_f with standard deviation $\sqrt{1/2c_f}$. The fringe width is given by $2\pi/k_f$. The visibility of the fringe and phase shift are determined from v_f and ϕ_f respectively.

Phase shift, average intensity and visibility from the interferogram: From the interference pattern obtained in the noncollinear displaced Sagnac interferometer, we determine the phase shift, the visibility, and the average intensity for different polarization states prepared by different combination of HWP and QWP angles (α, β) as shown in Fig. 3. The error bars in the plots are obtained from statistics over the 100 slices for the 5 images. In absence of QWP, the experimentally obtained value of phase is expected to be a constant with respect to α. This is considered as the zero reference for all the measurements. The mean and standard deviations associated with phase are obtained from the experimental datasets using circular statistics [42]. The phase shift obtained from the interferogram has more error
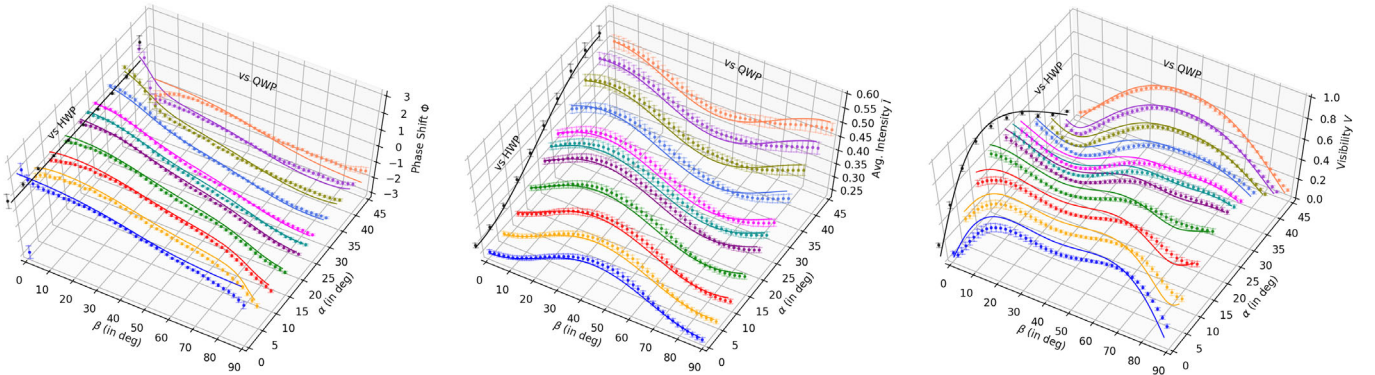

FIG. 3. Phase shift, avg. intensity, and visibility as a function of α and β. The solid lines in the plots represent the theoretical prediction while the dots and bars represent experimentally obtained mean and statistical error, respectively. The black curve (in the $\beta = 0$ plane) is for the experiment where only HWP was rotated in the absence of the QWP.

when θ is closer to 0 or π, since the Bloch vector is closer to the poles where ϕ is undefined, which is manifested in noticeable deviations from the theory in the experimental plot for HWP angles 0° and 45°.

All the experimentally obtained averaged intensity are normalized (with norm = 0.5) with respect to the corresponding maximum of the average intensity obtained as a function of HWP in the absence of QWP. The average intensity does not depend on the interference and hence is not prone to errors that affect the visibility and the phase shift. The experimentally obtained visibility is systematically lower than the theoretical prediction because of various experimental imperfections like polarization dependence of splitting ratio of the beam splitter (about 3%), angular deviation due to the rotation of the wave plates (10 arcsec) that changes the spatial overlap, and the intensity averaging over the pixel area.

Assuming that the polarization state of the incident beam is pure, we compute the fidelity of the state reconstructed from θ and ϕ determined by the experimentally obtained average intensity $\bar{I}$ and phase shift Φ, respectively. The errors obtained in Φ and $\bar{I}$ are propagated to the calculation of fidelity for a single state. The mean fidelity calculated from experimentally obtained mean phase shift (Φ) and mean average intensity ($\bar{I}$) are plotted on the Bloch sphere at the θ and ϕ of the prepared state in Fig. 4 (left) with the values indicated by the color bar. The average fidelity over all the prepared states is greater than 98%.

Although the incident state was almost pure ($> 99\%$ vertically polarized), our method can be used in experiments involving mixed states as well. To illustrate, we reconstruct the density matrix, as given in Eq. (1) using the μ value determined from the experimentally obtained visibility, with the restriction that it makes the reconstructed density matrix physical, i.e., $\text{Tr}(\rho^2) \le 1$. This is ensured by construction of ρ in Eq. (1) with the restriction that we substitute μ with $\min(\mu, 1)$ as discussed in detail in the Supplemental Material, Sec. VII [37]. Since the experimentally obtained visibility is systematically lower than the theory, the reconstructed state has a lower purity and, consequently, the fidelity [in Fig. 4 (right)] is lower than the case with pure state assumption.

Quantum state interferography for qudit pure states.— The pure state of a d-dimensional qudit can be represented in the polar spherical [43] form as follows:

$$|\psi\rangle^{(d)} = \begin{pmatrix} \cos(\theta_1/2) \\ \sin(\theta_1/2)\exp(i\phi_1)\cos(\theta_2/2) \\ \vdots \\ \prod_{j=1}^{k-1}\sin(\theta_j/2)\exp(i\phi_j)\cos(\theta_k/2) \\ \vdots \\ \prod_{j=1}^{d-1}\sin(\theta_j/2)\exp(i\phi_j) \end{pmatrix}. \quad (7)$$
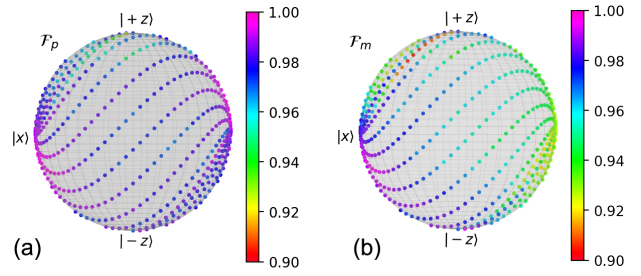

FIG. 4. (Left) Fidelity with assumption that the various prepared states in θ and ϕ over the Bloch sphere are pure. (Right) Fidelity of reconstructed density matrices of various prepared states in θ and ϕ over the Bloch sphere.

The component of $|\psi\rangle^{(d)}$ in the kth two-dimensional subspace is given by

$$|\psi\rangle_k^{(2;d)} = \left(\prod_{j=1}^{k-1}\sin\left(\frac{\theta_j}{2}\right)e^{i\phi_j}\right)\begin{pmatrix} \cos\left(\frac{\theta_k}{2}\right) \\ \sin\left(\frac{\theta_k}{2}\right)e^{i\phi_k}\cos\left(\frac{\theta_{k+1}}{2}\right) \end{pmatrix}. \quad (8)$$

We use $d-1$ interferometers, one on each of the two-dimensional $\{k, k+1\}$ subspaces of the d-dimensional state $|\psi\rangle^{(d)}$. The expectation values of σ_- and Π_0 operators for the two-dimensional subspace can be obtained directly from phase averaged intensity and phase shift of the interference pattern. Although, here we shall be formulating QSI for qudits using $d-1$ interferometers for ease of conceptualization, in principle and in many physical systems in practice, the state can be inferred from $d-1$ interferograms obtained with a setup involving only two interferometers. This is achieved by using the same interferometer for all the two-dimensional subspaces (see Supplemental Material, Sec. XIII [37]).

The matrix element of the spin ladder operator [44] in the two-dimensional subspace is

$$\langle\psi|\sigma_\pm^{(k)}|\psi\rangle_k^{(2;d)} = \xi(k)\frac{1}{2}e^{\pm i\phi_k}\sin(\theta_k)\cos\left(\frac{\theta_{k+1}}{2}\right), \quad (9)$$

where, $\xi(k) = \prod_{j=1}^{k-1}\sin^2(\theta_j/2)$.

We directly obtain the relative phase ϕ_k in the two-dimensional subspace from the argument of the matrix element of the spin ladder operator in that subspace. To determine θ_k, however, we need to know $\xi(k)$ and θ_{k+1} as well. Nevertheless, as in the case for qubits, we need to measure the matrix element of $\Pi_0^{(k)}$ in the two-dimensional subspace, i.e.,

$$\langle\psi|\Pi_0^{(k)}|\psi\rangle_k^{(2;d)} = \xi(k)\cos^2\left(\frac{\theta_k}{2}\right). \quad (10)$$

We can determine θ_1 and, subsequently, θ_2 as follows:

$$\frac{\theta_1}{2} = \cos^{-1}(\sqrt{\langle\Pi_0^{(1)}\rangle}), \qquad \frac{\theta_2}{2} = \cos^{-1}\left(\frac{2|\langle\sigma_\pm^{(1)}\rangle|}{\sin(\theta_1)}\right). \quad (11)$$
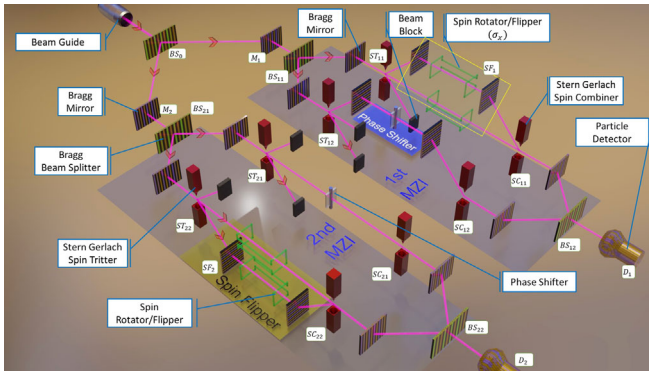
FIG. 5. Schematic to measure the state for a qutrit, which can be generalized to any qudit: The beam is divided into $d-1$ spatial modes. Each mode is made incident on an interferomter with $\Pi_0^{(k)}$ and $\sigma_x^{(k)}$ operations corresponding to the two-dimensional subspace (For a detailed description see Supplemental Material, Sec. XI [37]).

Thus, once θ_k is determined, θ_{k+1} can be obtained sequentially.

We can employ the same scheme to obtain $\langle \sigma_\pm^{(k)} \rangle$ by placing the polar decomposed elements $\Pi_0^{(k)}$ in one and $\sigma_x^{(k)}$ in the other arm of a MZI constructed for the two-dimensional subspace $\{k, k+1\}$. We have to design $d-1$ such MZI setups for the state estimation of a d-dimensional qudit.

Next, we present a generic scheme to construct all the necessary operators in each subspace from the Pauli operators in the d-dimensional Hilbert space. We illustrate the same using the example of qutrits in Fig. 5.

This scheme can be generalized with d dimensions simply by blocking all other components after the spin splitter (ST) except the desired pair. See Supplemental Material Sec. XII [37] for detailed expressions on how to infer the state from $d-1$ interferograms, which is also shown to be obtained with two interferometers in Sec. XIII.

Conclusions and outlook.—In summary, we have proposed quantum state interferography as a method to reconstruct a qubit state, whether pure or mixed, in a single experimental setup, and experimentally demonstrated our scheme with high average fidelity. This forms an efficient scheme compared to quantum state tomography as well as direct measurement techniques to infer the state of an ensemble of identically prepared qubits.

All the parameters needed to determine the state are obtained from the interference pattern produced using a single-shot measurement. Since the interference pattern obtained using the coherent laser light source and a stream of single photons would be identical [45,46], the method described here is applicable for determining the state of an identically prepared ensemble of single photons as well. QSI provides us with a "black box" approach to quantum state estimation, wherein, between the incidence of the photon and extraction of state information, we are not changing any conditions within the setup, which itself can be miniaturized. This provides us a true single shot estimation of the quantum state which has a rich potential for future technological development.

We have also shown here how QSI can be extended to estimate pure states of d-dimensional qudits with $d-1$ measurements, which can be obtained either by using $d-1$ interferometers as shown in Fig. 5 or by using only two interferometers as shown in accompanying Supplemental Material [37]. This is achieved by representing a d-dimensional qudit using $2(d-1)$ parameters and extracting 2 parameters from each interferogram. While for qubits we require one measurement as opposed to three in standard QST, the improvement is even more tremendous for qudits where standard quantum state tomography, without any assumptions, scales roughly as d^2 and for pure states, the scaling has been brought down to $5d-7$ [6,7] so far. This may help in efficient characterization of higher-dimensional systems [47] aimed towards quantum information processing, quantum computation, and quantum communication. The QSI can also be used for single-shot entanglement quantification of pure bipartite states, which can be useful towards foundation of quantum mechanics.

*usinha@rri.res.in

[1] S. M. Barnett and S. Croke, Quantum state discrimination, Adv. Opt. Photonics 1, 238 (2009).

[2] E. Toninelli, B. Ndagano, A. Valls, B. Sephton, I. Nape, A. Ambrosio, F. Capasso, M. J. Padgett, and A. Forbes, Concepts in quantum state tomography and classical implementation with intense light: A tutorial, Adv. Opt. Photonics 11, 67 (2019).

[3] K. Banaszek, M. Cramer, and D. Gross, Focus on quantum tomography, New J. Phys. 15, 125020 (2013).

[4] D. F. V. James, P. G. Kwiat, W. J. Munro, and A. G. White, Measurement of qubits, Phys. Rev. A 64, 052312 (2001).

[5] K. Banaszek, G. M. DAriano, M. G. A. Paris, and M. F. Sacchi, Maximum-likelihood estimation of the density matrix, Phys. Rev. A 61, 010304(R) (1999).

[6] J. Chen, H. Dawkins, Z. Ji, N. Johnston, D. Kribs, F. Shultz, and B. Zeng, Uniqueness of quantum states compatible with given measurement results, Phys. Rev. A 88, 012109 (2013).

[7] X. Ma, T. Jackson, H. Zhou, J. Chen, D. Lu, M. D. Mazurek, K. A. G. Fisher, X. Peng, D. Kribs, K. J. Resch, Z. Ji, B. Zeng, and R. Laflamme, Pure-state tomography with the expectation value of pauli operators, Phys. Rev. A 93, 032140 (2016).

[8] M. Cramer, M. B. Plenio, S. T. Flammia, R. Somma, D. Gross, S. D. Bartlett, O. Landon-Cardinal, D. Poulin, and Y.-K. Liu, Efficient quantum state tomography, Nat. Commun. 1, 149 (2010).

 [9] B. Qi, Z. Hou, L. Li, D. Dong, G. Xiang, and G. Guo, Quantum state tomography via linear regression estimation, Sci. Rep. **3**, 3496 (2013).

[10] J. J. Daz, I. Sainz, and A. B. Klimov, Quantum tomography via nonorthogonal basis and weak values, Phys. Rev. A **91**, 062127 (2015).

[11] A. Di Lorenzo, Quantum state tomography from a sequential measurement of two variables in a single setup, Phys. Rev. A **88**, 042114 (2013).

[12] M.-W. Lin and I. Jovanovic, Single-shot measurement of temporally-dependent polarization state of femtosecond pulses by angle-multiplexed spectral-spatial interferometry, Sci. Rep. **6**, 32839 (2016).

[13] Z. Zhu, D. Hay, Y. Zhou, A. Fyffe, B. Kantor, G. S. Agarwal, R. W. Boyd, and Z. Shi, Single Shot Direct Tomography of the Complete Transverse Amplitude, Phase, and Polarization Structure of a Light Field, Phys. Rev. Applied **12**, 034036 (2019).

[14] Athira B S, M. Pal, S. Mukherjee, J. Mishra, D. Nandy, and N. Ghosh, Single-shot measurement of the space-varying polarization state of light through interferometric quantification of the geometric phase, Phys. Rev. A **101**, 013836 (2020).

[15] A. Di Lorenzo, Sequential Measurement of Conjugate Variables as an Alternative Quantum State Tomography, Phys. Rev. Lett. **110**, 010404 (2013).

[16] S. Wu, State tomography via weak measurements, Sci. Rep. **3**, 1193 (2013).

[17] X. Chen, H.-Y. Dai, L. Yang, and M. Zhang, Alternative method of quantum state tomography toward a typical target via a weak-value measurement, Phys. Rev. A **97**, 032120 (2018).

[18] E. Shojaee, C. S. Jackson, C. A. Riofrío, A. Kalev, and I. H. Deutsch, Optimal Pure-State Qubit Tomography via Sequential Weak Measurements, Phys. Rev. Lett. **121**, 130404 (2018).

[19] Y. Aharonov, D. Z. Albert, and L. Vaidman, How the Result of a Measurement of a Component of the Spin of a Spin-1/2 Particle can Turn Out to be 100, Phys. Rev. Lett. **60**, 1351 (1988).

[20] I. M. Duck, P. M. Stevenson, and E. C. G. Sudarshan, The sense in which a "weak measurement" of a spin-1/2 particle's spin component yields a value 100, Phys. Rev. D **40**, 2112 (1989).

[21] J. S. Lundeen, B. Sutherland, A. Patel, C. Stewart, and C. Bamber, Direct measurement of the quantum wavefunction, Nature (London) **474**, 188 (2011).

[22] J. S. Lundeen and C. Bamber, Procedure for Direct Measurement of General Quantum States Using Weak Measurement, Phys. Rev. Lett. **108**, 070402 (2012).

[23] G. S. Thekkadath, L. Giner, Y. Chalich, M. J. Horton, J. Banker, and J. S. Lundeen, Direct Measurement of the Density Matrix of a Quantum System, Phys. Rev. Lett. **117**, 120401 (2016).

[24] J. Z. Salvail, M. Agnew, A. S. Johnson, E. Bolduc, J. Leach, and R. W. Boyd, Full characterization of polarization states of light via direct measurement, Nat. Photonics **7**, 316 (2013).

[25] M. Malik, M. Mirhosseini, M. P. J. Lavery, J. Leach, M. J. Padgett, and R. W. Boyd, Direct measurement of a 27-dimensional orbital-angular-momentum state vector, Nat. Commun. **5**, 3115 (2014).

[26] M. Mirhosseini, O. S. Magaña-Loaiza, S. M. Hashemi Rafsanjani, and R. W. Boyd, Compressive Direct Measurement of the Quantum Wave Function, Phys. Rev. Lett. **113**, 090402 (2014).

[27] Zhimin Shi, M. Mirhosseini, J. Margiewicz, M. Malik, F. Rivera, Ziyi Zhu, and R. W. Boyd, Direct measurement of an one-million-dimensional photonic state, in *2016 Progress in Electromagnetic Research Symposium (PIERS)* (2016), pp. 187–187.

[28] G. Nirala, S. N. Sahoo, A. K. Pati, and U. Sinha, Measuring average of non-hermitian operator with weak value in a Mach-Zehnder interferometer, Phys. Rev. A **99**, 022111 (2019).

[29] A. A. Abbott, R. Silva, J. Wechs, N. Brunner, and C. Branciard, Anomalous weak values without post-selection, Quantum **3**, 194 (2019).

[30] K. Ogawa, O. Yasuhiko, H. Kobayashi, T. Nakanishi, and A. Tomita, A framework for measuring weak values without weak interactions and its diagrammatic representation, New J. Phys. **21**, 043013 (2019).

[31] A. K. Pati, U. Singh, and U. Sinha, Measuring non-Hermitian operators via weak values, Phys. Rev. A **92**, 052120 (2015).

[32] E. Bolduc, G. Gariepy, and J. Leach, Direct measurement of large-scale quantum states via expectation values of non-Hermitian matrices, Nat. Commun. **7**, 10439 (2016).

[33] Here, by single shot, we mean that the measurement settings do not change during the course of data acquisition.

[34] F. Flamini, N. Spagnolo, and F. Sciarrino, Photonic quantum information processing: A review, Rep. Prog. Phys. **82**, 016001 (2019).

[35] S. Slussarenko and G. J. Pryde, Photonic quantum information processing: A concise review, Appl. Phys. Rev. **6**, 041303 (2019).

[36] M. Miuda, E. Dolkov, I. Straka, M. Mikov, M. Duek, J. Fiurek, and M. Jeek, Highly stable polarization independent Mach-Zehnder interferometer, Rev. Sci. Instrum. **85**, 083103 (2014).

[37] See Supplemental Material at http://link.aps.org/supplemental/10.1103/PhysRevLett.125.123601 for derivation and for a comparison between interferometers for QSI, which includes Ref. [38]; the state reconstruction of bipartite qubit pure states is detailed in Sec. XIV; Sec. VIII details how μ affects the fidelity and other methods to obtain μ from experiment that makes ρ physical is discussed; see Sec. XIII.

[38] S. P. Walborn, M. O. Terra Cunha, S. Pádua, and C. H. Monken, Double-slit quantum eraser, Phys. Rev. A **65**, 033818 (2002).

[39] C. H. Bennett, H. J. Bernstein, S. Popescu, and B. Schumacher, Concentrating partial entanglement by local operations, Phys. Rev. A **53**, 2046 (1996).

[40] R. Horodecki, P. Horodecki, M. Horodecki, and K. Horodecki, Quantum entanglement, Rev. Mod. Phys. **81**, 865 (2009).

[41] R. D. Sorkin, On the Entropy of the Vacuum Outside a Horizon, in *General Relativity and Gravitation* edited by B. Bertotti, F. de Felice, and A. Pascolini (1983), Vol. 1, p. 734.

[42] N. I. Fisher, *Statistical Analysis of Circular Data* (Cambridge University Press, 1993).

[43] L. E. Blumenson, A derivation of n-dimensional spherical coordinates, Am. Math. Mon. **67**, 63 (1960).

[44] We shall use the notation $\mathcal{O}^{(k)}$ to denote the operator $\mathcal{O}$ meant for qubits realized in the kth two-dimensional subspace. The operators for d-dimensional qudits are represented as $\mathcal{O}^{[k]}$.

[45] B.-S. K. Skagerstam, On the three-slit experiment and quantum mechanics, J. Phys. Commun. **2**, 125014 (2018).

[46] E. C. G. Sudarshan, Equivalence of Semiclassical and Quantum Mechanical Descriptions of Statistical Light Beams, Phys. Rev. Lett. **10**, 277 (1963).

[47] D. Ghosh, T. Jennewein, P. Kolenderski, and U. Sinha, Spatially correlated photonic qutrit pairs using pump beam modulation technique, OSA Continuum **1**, 996 (2018).